DALTON
FULL PAPER

Syntheses, crystal structures and non-linear optical properties of two novel windmill-shaped clusters: $[M_2Pd_4S_8(dppm)_2]\cdot 4DMF$ (M = W or Mo)

Hegen Zheng,[a] Wa-Hung Leung,[b] Weilian Tan,[c] Deliang Long,[d] Wei Ji,[c] Jiutong Chen,[d] Feibo Xin[a] and Xinquan Xin*[a]

[a] *State Key Laboratory of Coordination Chemistry, Coordination Chemistry Institute, Nanjing University, Nanjing, 210093, P.R. China. E-mail: xxin@netra.nju.edu.cn*
[b] *Department of Chemistry, The Hong Kong University of Science and Technology, Clear Water Bay, Kowloon, Hong Kong*
[c] *Department of Physics, National University of Singapore, Singapore 119260, Republic of Singapore*
[d] *State Key Laboratory of Structural Chemistry, Fujian Institute of Research on Structure of Matter, Chinese Academy of Sciences, Fuzhou, Fujian 350002, P. R. China*

Received 24th January 2000, Accepted 20th April 2000
Published on the Web 8th June 2000

Novel cluster compounds $[M_2Pd_4S_8(dppm)_2]\cdot 4DMF$ (M = W **1** or Mo **2**) were synthesized by the reaction of $[NEt_4]_2[MS_4]$ and $[Pd(dppm)Cl_2]$ (dppm = $Ph_2PCH_2PPh_2$) in CH_2Cl_2 and CH_3CN, and their crystal structures have been characterized by X-ray diffraction. Both clusters have novel new skeletal structures with eight atoms in a plane. The non-linear optical properties of **1** were studied with a 7 ns pulsed laser at 532 nm. The effective third-order non-linearities were determined yielding $\alpha_2 = 1.2 \times 10^{-6}$ cm W^{-1} M^{-1} and $n_2 = -1.5 \times 10^{-10}$ cm^2 W^{-1} M^{-1}. Compound **1** exhibits a considerably large self-defocusing property.

Introduction

The tetrathiometalate anions MoS_4^{2-} (WS_4^{2-}), VS_4^{3-} and ReS_4^- play a key role in some biological processes and industrial catalyses as well as the syntheses of new materials.[1–4] The synthetic and structural chemistry of heterometallic sulfide clusters containing d^{10} copper(I) and silver(I) has been developed rapidly, and some interesting Mo(W)/Cu(Ag)/S clusters with novel structural types have been synthesized.[5–10] In our search for better non-linear optical (NLO) materials we have undertaken a series of studies on structures and NLO properties.[11–16] Together with our effort on the design of Group 6–Group 10 mixed-metal sulfido complexes, this prompted us to extend our studies to heterometallic sulfido clusters derived from MS_4^{2-} (M = Mo or W) with palladium. The structural characterization of Mo(W)/Pd/S clusters may help us to understand more about their NLO properties. However, no heterosulfidometallic clusters containing Pd^I has been reported, besides a few interesting studies on Mo(W)/Pd/S complexes containing Pd^0 and Pd^{II}.[17–20] Here the syntheses and structural characterizations of the two new hexanuclear clusters $[W_2Pd_4S_8(dppm)_2]\cdot 4DMF$ **1** and $[Mo_2Pd_4S_8(dppm)_2]\cdot 4DMF$ **2** are reported for the first time, and non-linear optical properties of **1** are also studied.

Experimental

The compounds $[NEt_4]_2[MS_4]$ (M = W or Mo) and $[Pd(dppm)Cl_2]$ were prepared according to the literature.[21,22] Other chemicals were of A.R. grade and used without further purification.

Physical measurements

Infrared spectra were recorded on a Fourier Nicolet FT-170SX spectrophotometer with pressed KBr pellets and linear absorption spectra with a Hitachi U-3410 spectrophotometer. Carbon and hydrogen analyses were performed on a PE 240C Elemental Analyser. NMR spectra were recorded on a Bruker ALX300 spectrometer in $CDCl_2$ solvent.

Non-linear optical (NLO) measurements

A dimethylformamide (DMF) solution of compound **1** with concentration of 1.7×10^{-3} M contained in a 1 mm thick quartz cuvette was irradiated by a Q-switched frequency-doubled Nd:YAG laser, which produced linearly polarized 7 ns (full width at half maximum, FWHM) optical pulses at 532 nm. The laser was operated at a pulse repetition rate of 10 Hz. The spatial profiles of the optical pulses were nearly Gaussian after passing through a filter. The laser beam was then divided by a beam splitter into two parts: one was used as a reference for the incident energy and the other focused onto the sample by a mirror of 25 cm focal length. The minimum beam radius of the focused laser beam was measured to be 30 ± 5 μm. Incident and transmitted pulse energies were measured simultaneously by two energy detectors (Rjp-735 energy probes, Laser Precision) linked to a computer by an IEEE interface. The NLO properties of the sample were determined by performing *Z*-scan measurements.[23] The sample was mounted on a translation stage that was controlled by the computer to move along the *Z* axis with respect to the focal point. For determining both the sign and magnitude of the non-linear refraction, a 1.0 mm diameter aperture was placed in front of the transmission detector and the transmittance recorded as a function of the sample position on the *Z* axis (closed-aperture *Z* scan). For measuring the non-linear absorption, the *Z*-dependent sample transmittance was taken without the aperture (open-aperture *Z* scan).

Synthesis of $[W_2Pd_4S_8(dppm)_2]\cdot 4DMF$ 1

A solution of $[NEt_4]_2[WS_4]$ (0.286 g, 0.5 mmol) in 30 ml of CH_2Cl_2 and CH_3CN (1 : 1 v/v) was added to $[Pd(dppm)Cl_2]$

DOI: 10.1039/b000616p

(0.250 g, 0.5 mmol) and stirred for 12 h at room temperature and then filtered. The obtained solid was dissolved in 2 ml of DMF and then filtered, diethyl ether added to the resulting filtrate and the obtained dark crystals were isolated after a week (0.32 g, yield 61%). Found: C, 35.24; H, 3.47; N, 2.68. Calc.: C 35.28, H, 3.44; N, 2.65%. IR spectrum (KBr pellets): ν(W–S) 484.5s, 441.7s and 413.6m cm^{-1}. ^1H NMR (TMS as standard): δ 8.00 (s, 4 H), 7.10–7.40 (m, 40 H), 3.50–3.73 (m, 4 H), 2.97 (s, 12 H) and 2.83 (s, 12 H).

Synthesis of $[Mo_2Pd_4S_8(dppm)_2]\cdot 4DMF$ 2

A procedure similar to that above was employed with $[NEt_4]_2[MoS_4]$ (0.242 g, 0.5 mmol) instead of $[NEt_4]_2[WS_4]$. Black crystals were obtained by allowing Et_2O to diffuse into the dark filtrate at room temperature for several days (0.33 g, yield 67%). The compound is slightly soluble in DMF. Found: C, 38.12; H, 3.83; N, 2.81. Calc.: C, 38.45; H, 3.75; N, 2.89%. IR spectrum (KBr pellets): ν(Mo–S) 507.5s, 460.2s and 451.1m cm^{-1}. ^1H NMR (TMS as standard): δ 8.04 (s, 4 H), 7.12–7.38 (m, 40 H), 3.53–3.70 (m, 4 H), 2.99 (s, 12 H) and 2.84 (s, 12 H).

Crystal structure analysis

The raw data for compounds **1** and **2** were collected on a Siemens SMART CCD area-detecting diffractometer. The structures were solved with the SHELXTL program[24] and refined by full-matrix least-squares methods based on F^2, with anisotropic thermal parameters for the non-hydrogen atoms. The hydrogen atoms were located theoretically and refined in the final stages with a restrained geometry (C–H 0.95 Å) and common isotropic displacement parameter. Hydrogen atoms were located theoretically and not refined. Crystal data are summarized in Table 1.

CCDC reference number 186/1944.

See http://www.rsc.org/suppdata/dt/b0/b000616p/ for crystallographic files in .cif format.

Results and discussion

Synthesis of clusters 1 and 2

Reaction of $[Pd(dppm)Cl_2]$ with $[NEt_4]_2[MS_4]$ (M = W or Mo) in the molar ratio of 1 : 1 in CH_2Cl_2–CH_3CN (1 : 1 v/v) at ambient temperature in the air, followed by recrystallization from DMF–Et_2O, gave the hexanuclear compounds **1** and **2** as black crystals. However, it is notable that $M_2Pd_4S_8$ (M = W or Mo) core clusters with dppe ligands cannot be prepared in a similar reaction; only binuclear compounds $[MPdS_4(dppe)]$ (M = W or Mo) were obtained,[20] which show that dppm as a bidentate ligand in the present reaction played an important role to bridge the two palladium(I) atoms (Scheme 1).

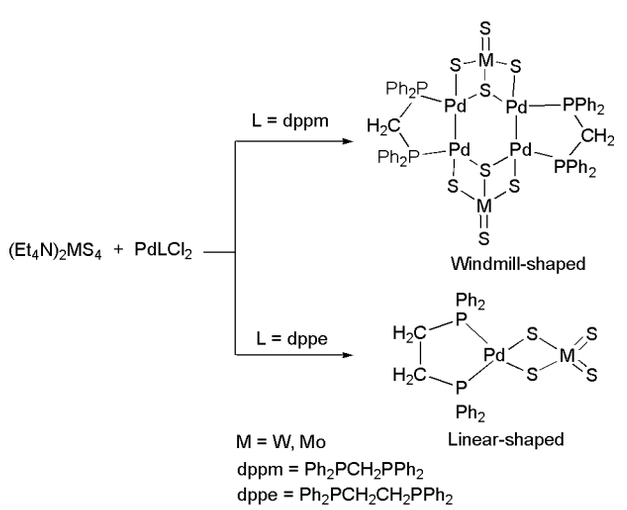

Scheme 1

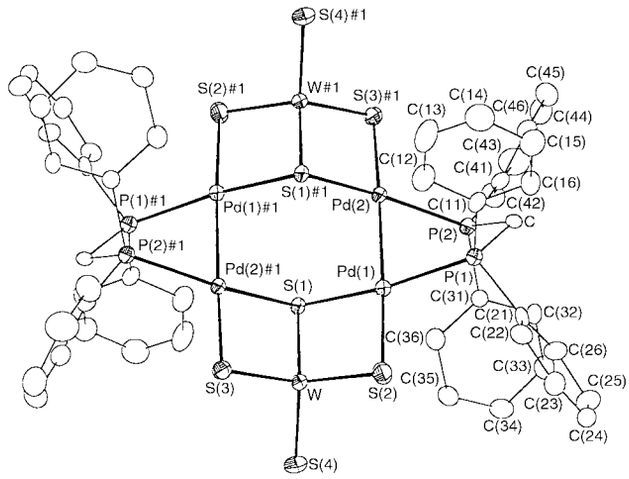

Fig. 1 The crystal structure of $[W_2Pd_4S_8(dppm)_2]$.

Crystal structures of clusters 1 and 2

The two compounds are isomorphous and crystallize in the monoclinic space group $P2_1/n$ with two molecules in a unit cell. Therefore, the structure of **1** will be mainly described. It is a neutral cluster with four solvent molecules. The structure of $[W_2Pd_4S_8(dppm)_2]$ which is situated on a crystallographic inversion center is shown in Fig. 1. It can be seen that a plane of four Pd atoms, symmetrically disposed around the inversion center, is "glued" together by two μ_3-WS_4^{2-} and two μ-dppm ligands. Each Pd atom has a square planar co-ordination geometry, bound to two S atoms from WS_4^{2-}, one P atom from dppm and another Pd atom. Such an arrangement of the palladium atoms seems to be very much dependent on the nature of the auxiliary ligands. Within the cluster, four Pd and two μ_3-S atoms form a six-membered Pd_4S_2 ring which seems to be stabilized by two distorted five-membered Pd_2P_2C rings formed by a μ-dppm ligand and Pd–Pd bond; thus, a cavity exists inside the cluster molecule. Charge balance suggests that compound **1** contains the formal oxidation states Pd^{I} and W^{VI}. The Pd^{I}–Pd^{I} distance of 2.5930(8) Å in **1** is obviously shorter than those of 2.623(1) and 2.625(2) Å in $[Pd_2(pyphos)_2(Hpyphos)_2]$[25] (pyphos = 6-(diphenylphosphino)-2-pyridonate) and $[Pd_2(\mu\text{-}Br)_2(PBu^t_3)_2]$,[26] respectively, which may indicate strong Pd^{I}–Pd^{I} interactions, since the Pd–Pd distance in metallic palladium is 2.82(2) Å.[27] Little variations in S_{bridge}–W–$S_{terminal}$ (110.18(10)–111.66(9)°) and S_{bridge}–W–S_{bridge} (106.54(7)–110.97(9)°) angles show that co-ordination of the W is essentially tetrahedral. The W–S bond lengths fall into three categories: the distance between terminal S and W atoms is 2.133(2) Å; an average W–μ-S distance of 2.208(2) Å is shorter than the W–μ_3-S distance of 2.274(2) Å. However, it is interesting that the Pd-μ_3-S distance of 2.362(2) Å is significantly shorter than the Pd-μ-S distance of 2.376(2) Å, this together with elongation of W–μ_3-S suggesting that conjugate stress of the W–S–Pd groups results in the W–μ_3-S bond being weakened and the Pd-μ_3-S bond being strengthened.

Interestingly, S(2), Pd(1), Pd(2) and S(3)#1 atoms are approximately collinear because of the S(2)–Pd(1)–Pd(2) and Pd(1)–Pd(2)–S(3)#1 angles of 176.64(7) and 176.07(6)°, moreover those four atoms and their symmetry related S(2)#1, Pd(1)#1, Pd(2)#1 and S(3) are nearly coplanar with deviations of not more than 0.053 Å from the least squares plane. The two W atoms deviate 1.57 Å from this eight-atom plane. The average $W\cdots Pd^{I}$ distance of 2.8723 Å in **1** is slightly shorter than the $W\cdots Pd^{II}$ distance of 2.887(2) Å observed in $[PdWS_4(dppe)]$,[20] while the average $Mo\cdots Pd^{I}$ distance of 2.8548(12) Å in **2** is obviously longer than the Mo–Pd^{0} distances of 2.793(3) and 2.799(2) Å in $[Pd_2Mo_3S_4(tacn)_3Cl]Cl_3$ (tacn = 1,4,7-triazacyclononane) and $[Pd_2Mo_6S_8(H_2O)_{18}][OTs]_8$ (OTs = *p*-toluenesulfonate) respectively.[19] The important bond lengths and bond angles are listed in Tables 2 and 3.

Table 1 Crystal data, data collection and structure refinement parameters for $[W_2Pd_4S_8(dppm)_2]\cdot 4DMF$ **1** and $[Mo_2Pd_4S_8(dppm)_2]\cdot 4DMF$ **2**

	1	**2**
Empirical formula	$C_{62}H_{72}N_4O_4P_4Pd_4S_8W_2$	$C_{62}H_{72}Mo_2N_4O_4P_4Pd_4S_8$
Formula weight	2110.90	1935.08
Crystal system	Monoclinic	Monoclinic
Space group	$P2_1/n$ (no. 13)	$P2_1/n$ (no. 13)
a/Å	13.0822(3)	13.0593(2)
b/Å	19.6074(3)	19.5518(4)
c/Å	14.4743(3)	14.4955(2)
β/°	97.12(1)	97.1080(10)
V/Å^3	3684.11(13)	3672.73(11)
Z	2	2
μ/mm^{-1}	4.425	1.650
T/K	293(2)	293(2)
Reflections collected	13223	13177
Independent reflections	6204 (R_{int} = 3.97%)	6194 (R_{int} = 7.87%)
Observed reflections	4847 ($I > 2.0\sigma(I)$)	3564 ($I > 2.0\sigma(I)$)
Data/restraints/parameters	6202/0/397	6191/0/397
Final $R1$, $wR2$ indices ($I > 2\sigma(I)$)	0.0441, 0.0833	0.0691, 0.1541

Table 2 Bond lengths (Å) and bond angles (°) for compound **1**

W–S(4)	2.133(2)	W–S(2)	2.203(2)
W–S(3)	2.213(2)	W···Pd(1)	2.8756(7)
W–S(1)	2.274(2)	W···Pd(2)#1	2.8690(6)
Pd(1)–S(2)	2.376(2)	Pd(2)–S(1)#1	2.348(2)
Pd(1)–P(1)	2.273(2)	Pd(1)–S(1)	2.363(2)
Pd(1)–Pd(2)	2.5930(8)	Pd(2)–P(2)	2.268(2)
Pd(2)–S(3)#1	2.373(2)	Pd(2)···W#1	2.8689(6)
S(3)–Pd(2)#1	2.373(2)	S(1)–Pd(2)#1	2.348(2)
S(4)–W–S(2)	110.18(10)	S(4)–W–S(3)	110.61(9)
S(2)–W–S(3)	110.97(9)	S(4)–W–S(1)	111.66(9)
S(2)–W–S(1)	106.78(7)	S(3)–W–S(1)	106.54(7)
S(4)–W–Pd(2)#1	129.15(7)	S(2)–W–Pd(2)#1	120.62(7)
S(3)–W–Pd(2)#1	53.81(6)	S(1)–W–Pd(2)#1	52.79(5)
S(4)–W–Pd(1)	130.04(7)	S(2)–W–Pd(1)	53.83(6)
S(3)–W–Pd(1)	119.32(6)	S(1)–W–Pd(1)	53.09(5)
Pd(2)#1–W–Pd(1)	82.81(2)	P(1)–Pd(1)–S(1)	165.47(8)
P(1)–Pd(1)–S(2)	94.69(8)	S(1)–Pd(1)–S(2)	98.64(7)
P(1)–Pd(1)–Pd(2)	86.45(6)	S(1)–Pd(1)–Pd(2)	80.56(5)
S(2)–Pd(1)–Pd(2)	176.64(7)	P(1)–Pd(1)–W	143.12(6)
S(1)–Pd(1)–W	50.29(5)	S(2)–Pd(1)–W	48.47(5)
Pd(2)–Pd(1)–W#1	130.43(3)	P(2)–Pd(2)–S(1)#1	160.63(8)
P(2)–Pd(2)–S(3)#1	96.36(8)	S(1)#1–Pd(2)–S(3)#1	99.27(7)
P(2)–Pd(2)–Pd(1)	83.44(6)	S(1)#1–Pd(2)–Pd(1)	81.74(5)
S(3)#1–Pd(2)–Pd(1)	176.07(6)	P(2)–Pd(2)–W#1	144.27(6)
S(1)#1–Pd(2)–W	50.48(5)	S(3)#1–Pd(2)–W#1	48.84(5)
Pd(1)–Pd(2)–W#1	131.88(3)	W–S(1)–Pd(2)#1	76.73(6)
W–S(1)–Pd(1)	76.62(6)	Pd(2)#1–S(1)–Pd(1)	107.52(8)
W–S(2)–Pd(1)	77.70(7)	W–S(3)–Pd(2)#1	77.36(7)

Symmetry operator: #1 = $-x$, $1-y$, $1-z$.

Table 3 Bond lengths (Å) and bond angles (°) for compound **2**

Mo–S(4)	2.123(3)	Mo–S(2)	2.205(3)
Mo–S(3)	2.211(3)	Mo–Pd(1)	2.8580(12)
Mo–S(1)	2.277(3)	Mo–Pd(2)#1	2.8516(12)
Pd(1)–S(2)	2.357(3)	Pd(2)–S(1)#1	2.336(3)
Pd(1)–P(1)	2.275(3)	Pd(1)–S(1)	2.350(3)
Pd(1)–Pd(2)	2.5989(11)	Pd(2)–P(2)	2.273(3)
Pd(2)–S(3)#1	2.359(3)	Pd(2)–Mo#1	2.8517(12)
S(3)–Pd(2)#1	2.359(3)	S(1)–Pd(2)#1	2.336(3)
S(4)–Mo–S(2)	110.59(14)	S(4)–Mo–S(3)	110.85(13)
S(2)–Mo–S(3)	110.52(13)	S(4)–Mo–S(1)	111.72(13)
S(2)–Mo–S(1)	106.53(10)	S(3)–Mo–S(1)	106.48(10)
S(4)–Mo–Pd(2)#1	129.09(11)	S(2)–Mo–Pd(2)#1	120.27(10)
S(3)–Mo–Pd(2)#1	53.76(8)	S(1)–Mo–Pd(2)#1	52.76(7)
S(4)–Mo–Pd(1)	129.93(11)	S(2)–Mo–Pd(1)	53.62(8)
S(3)–Mo–Pd(1)	119.18(9)	S(1)–Mo–Pd(1)	53.02(7)
Pd(2)#1–Mo–Pd(1)	82.92(3)	P(1)–Pd(1)–S(1)	165.08(10)
P(1)–Pd(1)–S(2)	94.22(11)	S(1)–Pd(1)–S(2)	99.49(10)
P(1)–Pd(1)–Pd(2)	86.80(8)	S(1)–Pd(1)–Pd(2)	79.86(7)
S(2)–Pd(1)–Pd(2)	176.51(9)	P(1)–Pd(1)–Mo	143.02(8)
S(1)–Pd(1)–Mo	50.71(7)	S(2)–Pd(1)–Mo	48.87(8)
Pd(2)–Pd(1)–Mo	130.18(4)	P(2)–Pd(2)–S(1)#1	160.14(11)
P(2)–Pd(2)–S(3)#1	96.37(10)	S(1)#1–Pd(2)–S(3)#1	99.96(10)
P(2)–Pd(2)–Pd(1)	83.29(8)	S(1)#1–Pd(2)–Pd(1)	81.19(7)
S(3)#1–Pd(2)–Pd(1)	176.08(9)	P(2)–Pd(2)–Mo#1	144.48(8)
S(1)#1–Pd(2)–Mo#1	50.89(7)	S(3)#1–Pd(2)–Mo#1	49.10(7)
Pd(1)–Pd(2)–Mo#1	131.77(4)	Mo–S(1)–Pd(2)#1	76.35(8)
Mo–S(1)–Pd(1)	76.27(9)	Pd(2)#1–S(1)–Pd(1)	107.54(11)
Mo–S(2)–Pd(1)	77.51(10)	Mo–S(3)–Pd(2)#1	77.13(9)

Symmetry operator: #1 = $-x$, $1-y$, $1-z$.

Non-linear optical (NLO) properties

The electronic spectrum of compound **1** in DMF is depicted in Fig. 2. It has relatively low linear absorption in the visible and near-IR region. The lowest absorption peak is located at 400 nm (3.1 eV). The NLO properties of compound **1** were revealed by using a Z-scan technique.[23] Its non-linear absorptive and refractive properties are depicted by the filled and open circles, respectively, in Fig. 3. The solid curves were generated theoretically using eqns. (1), (2) and (3) where Z is the distance of the sample from the focal point, α_0 and α_2 are the linear and non-linear absorption coefficients, respectively, L is the sample thickness, I_0 the peak irradiance at the focus, $Z_0 = \pi\omega_0^2/\lambda$ with ω_0 the spot radius of the beam at the focus, γ is the non-linear index that is due to the bound electronic effect, s is the linear aperture transmittance, τ is the temporal pulse width of the beam, T represents transmission, P is the total power of the beam, z is the position of the sample and λ the wavelength of the laser, r is the radial coordinate, t the time and t_0 the pulse width. The transmittance changes detected behind the aperture when both NLO absorptive and refractive properties are considered are described by eqn. (3) where $P_T(z,t) = \varepsilon_0 c n_0 \pi \int_0^{r_a} |E_a(r, t, z)|^2 r\,dr$ and $P_i(t) = (1/2) I_0 \pi \omega_0^2 \exp[-(t/t_0)^2]$, where c and ε_0 are the speed of light and the permittivity in vacuum, respectively, and n_0 is the linear refractive index of the sample. At the aperture, the electric component of the optical field is given by eqns. (4) and (5), where d is the distance between the aperture and focus, k is the magnitude of the wave vector in free space, r' refers to the radial coordinate at the aperture in the optical field and J_0 is the zeroth-order Bessel's function; $S = 1 - \exp[-2(r_a/\omega_a)^2]$ is the linear aperture transmittance.

$$T(z) = \frac{1}{\sqrt{\pi} q(z)} \int_{-\infty}^{+\infty} \ln[1 + q(z) e^{-\tau^2}] d\tau \quad (1)$$

$$q(z) = \int_0^{\infty} \int_0^{\infty} \alpha_2 \frac{I_0}{1 + (Z/Z_0)^2} e^{[-2(\gamma/\omega_0)^2 - (t/t_0)^2]} \frac{1 - e^{-\alpha_0 L}}{\alpha_0} r\,dr\,dt \quad (2)$$

$$T(z,s) = \int_{-\infty}^{+\infty} P_T(t) dt / S \int_{-\infty}^{+\infty} P_i(t) dt \quad (3)$$

Table 4 NLO parameters for cluster compounds

Compound	Structure	$10^{-3}\ \alpha_0/cm^{-1}\ M^{-1}$	$\alpha_2/cm\ W^{-1}\ M^{-1}$	$10^{10}\ n_2/cm^2\ W^{-1}\ M^{-1}$
$[W_2Pd_4S_8(dppm)_2]^a$	Windmill	2.10	1.2×10^{-6}	−1.5
$[MoCu_3OS_3I(py)_5]^b$	Nested	0.04	2.5×10^{-5}	−1.3
$[WCu_3OS_3I(py)_5]^b$	Nested	2.10	15.0×10^{-5}	16.0
$[NEt_4][Mo_2Cu_6O_2S_6I_6]^c$	Twin-nested	0.74	2.0×10^{-5}	−3.0
$[WCu_2OS_3(PPh_3)_3]^d$	Butterfly	2.50	—[e]	6.70

α_0 is the linear absorption coefficient; α_2 the non-linear absorption coefficient and n_2 the non-linear refractive index. [a] This work. [b] Ref. 31. [c] Ref. 32. [d] Ref. 33. [e] Negligible.

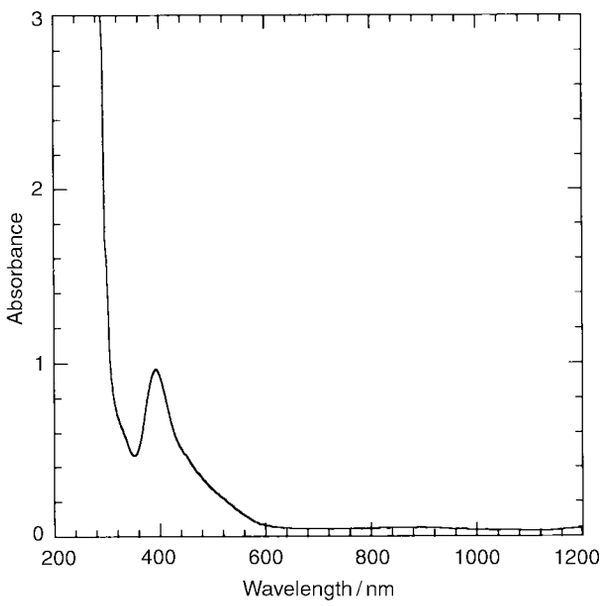

Fig. 2 Electronic spectrum of $[W_2Pd_4S_8(dppm)_2]$ (1.7×10^{-3} M) in DMF. The optical path is 1 mm.

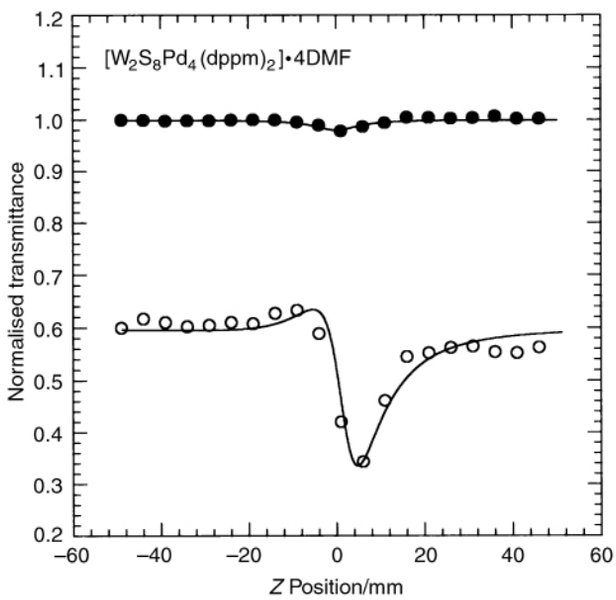

Fig. 3 The normalised Z-scan data $[W_2Pd_4S_8(dppm)_2]$ (1.7×10^{-3} M) in DMF solution with 532 nm, 7 ns laser pulses. The optical path is 1 mm. The peak incident irradiance of the pulses at the focus is 228 MW cm^{-2}. The experimental data were measured without (●) an aperture. The open circles (○) were obtained with the aperture and they have been vertically displaced by −0.4 for clarity. The solid curves are the theoretical fits based on Z-scan theory.

$$E_a(r, t, z) = \frac{2\pi}{i\lambda(d - z)} e^{i\pi r^2/\lambda(d - z)} \int_0^\infty r' E(r', t, z) e^{i\pi r^2/\lambda(d - z)} J_0 \frac{i\pi r r'}{\lambda(d - z)} dr \quad (4)$$

$$E(r', t, z) = 2\sqrt{\frac{I(r', t, z)}{\varepsilon_0 c n_0}} e^{\{(kn_2/\alpha_2)\ln[1 + q(r', t, z)]\}} \quad (5)$$

The good fits between the theory and our experimental data in Fig. 3 suggest that the observed NLO phenomena are effectively a third-order process. The effective α_2 and n_2 values are determined to be 1.2×10^{-6} cm W^{-1} M^{-1} and -1.5×10^{-10} cm^2 W^{-1} M^{-1}, respectively. In Fig. 3 it is observed that compound **1** shows a negative sign for n_2. This indicates that the laser beam propagating in it undergoes a self-defocusing process. This property shows that **1** can be a promising material for applications such as protection of optical sensors. Table 4 lists the measured non-linear absorption coefficient, α_2, and non-linear refractive index, n_2, for some cluster compounds. It should be noted that the Z-scan measurements reported here could not reveal the origin of the measured α_2 and n_2 values for **1**. Excited-state effects, two-photon absorption, third-order bound-electron effect and non-linear scattering are possible mechanisms behind the observed non-linearities.[28–30] Table 4 shows that **1** compares favorably with most of the other clusters in terms of the effective n_2 value.

Acknowledgements

This research was supported by the National Natural Science Foundation of China, the Hong Kong University of Science & Technology and National University of Singapore.

References

1 A. Müller, E. Diemann, R. Josters and H. Bögge, *Angew. Chem.*, 1981, **93**, 957; *Angew. Chem., Int. Ed. Engl.*, 1981, **20**, 934.
2 M. P. Croughan, *Molybdenum and Molybdenum-containing Enzymes*, Pergamon Press, Oxford, 1980.
3 A. Müller, E. Krickemeyer, A. Hildebrand, H. Bögge, K. Schneider and M. Lemke, *J. Chem. Soc., Chem. Commun.*, 1991, 1685.
4 J. T. Goodman and T. B. Rauchfuss, *Angew. Chem.*, 1997, **109**, 2173; *Angew. Chem., Int. Ed. Engl.*, 1997, **36**, 2083.
5 J. G. Li, X. Q. Xin, Z. Y. Zhou and K. B. Yu, *J. Chem. Soc., Chem. Commum.*, 1991, 249.
6 S. W. Du, N. Y. Zhu, P. C. Chen and X. T. Wu, *Angew. Chem.*, 1992, **104**, 1098; *Angew. Chem., Int. Ed. Engl.*, 1992, **31**, 1085.
7 E. A. Pruss, B. S. Snyder and A. M. Stacy, *Angew. Chem.*, 1993, **105**, 279; *Angew. Chem., Int. Ed. Engl.*, 1993, **32**, 256.
8 Q. Huang, X. T. Wu, Q. M. Wang, T. L. Sheng and J. X. Lu, *Angew. Chem.*, 1996, **108**, 985; *Angew. Chem., Int. Ed. Engl.*, 1996, **35**, 868.
9 Q. Huang, X. T. Wu, Q. M. Wang, T. L. Sheng and J. X. Lu, *Inorg. Chem.*, 1996, **35**, 893.
10 J. Guo, X. T. Wu, W. J. Zhang, T. L. Sheng, Q. Huang, P. Lin, Q. M. Wang and J. X. Lu, *Angew. Chem.*, 1997, **109**, 2574; *Angew. Chem., Int. Ed. Engl.*, 1997, **36**, 2464.
11 S. Shi, W. Ji, S. H. Tang, J. P. Lang and X. Q. Xin, *J. Am. Chem. Soc.*, 1994, **116**, 3651.
12 G. Salane, T. Shibahara, H. W. Hou, X. Q. Xin and S. Shi, *Inorg. Chem.*, 1995, **34**, 4785.
13 S. Shi, H. W. Hou and X. Q. Xin, *J. Phys. Chem.*, 1995, **99**, 4050.
14 S. Shi, Z. R. Chen, H. W. Hou, X. Q. Xin and K. B. Yu, *Chem. Mater.*, 1995, **7**, 1519.

15 H. G. Zheng, W. Ji, M. L. K. Low, G. Sakane, T. Shibahara and X. Q. Xin, *J. Chem. Soc.*, *Dalton Trans.*, 1997, 2357.
16 M. K. M. Low, H. W. Hou, H. G. Zheng, W. T. Wong, G. X. Jin, X. Q. Xin and W. Ji, *Chem. Commun.*, 1998, 505.
17 D. L. Long, W. T. Wong, S. Shi, X. Q. Xin and J. S. Huang, *J. Chem. Soc.*, *Dalton Trans.*, 1997, 4361.
18 K. E. Howard, T. B. Rauchfuss and S. R. Wilson, *Inorg. Chem.*, 1988, **27**, 3561.
19 T. Murata, Y. Mizobe, H. Gao, Y. Ishii, T. Wakabayashi, F. Nakano, T. Tanase, S. Yano, M, Hidai, I. Echizen, H. Nanikawa and S. Motomura, *J. Am. Chem. Soc.*, 1994, **116**, 3389.
20 B. Wu, W. J Zhang, X. Y. Huang, X. T. Wu and J. X. Lu, *Polyhedron.*, 1997, **16**, 801.
21 J. W. McDonald, G. D. Friesen, L. D. Rosenhein and W. E. Newton, *Inorg. Chim. Acta*, 1983, **72**, 205.
22 W. L. Steffen and G. J. Palenik, *Inorg. Chem.*, 1976, **15**, 2432.
23 M. Sheik-Bahae, A. A. Said, T. H. Wei, D. J. Hagan and E. W. Van Stryland, *IEEE J. Quantum Electron*, 1990, **26**, 760.
24 G. M. Sheldrick, SHELXTL, Version 5.0, Siemens Analytical X-Ray Instrumentation Inc., Madison, WI, 1994.
25 K. Mashima, M. Tanaka, K. Tani, H. Nakano and A. Nakamura, *Inorg. Chem.*, 1996, **35**, 5244.
26 G. M. Li, S. H. Li, A. L. Tan, W. H. Yip and T. C. W. Mak, *J. Chem. Soc.*, *Dalton Trans.*, 1996, 4315.
27 R. W. G. Wyckoff, *Crystal Structures*, *Vol. 1*, 2nd edn., Wiley, New York, 1963, p. 36.
28 W. Ji, W. Xie, S. H. Tang and S. Shi, *Mater. Chem. Phys.*, 1995, **43**, 1.
29 M. Sheik-Bahae, D. C. Hutching, D. J. Hagan and E. W. Van Stryland, *Phys. Rev. Lett.*, 1991, **65**, 96.
30 K. Mansour, M. J. Soileau and E. W. Van Stryland, *J. Opt. Soc. Am. B*, 1992, **9**, 1100.
31 P. Ge, W. Ji and S. Shi, *Inorg. Chem.*, 1996, **35**, 5363.
32 P. Ge, S. H. Tang, W. Ji, S. Shi, H. W. Hou, D. L. Long, X. Q. Xin, S. F. Lu and Q. J. Wu, *J. Phys. Chem. B*, 1997, **101**, 27.
33 H. W. Hou, X. Q. Xin, M. Q. Liu, M. Q. Chen and S. Shi, *J. Chem. Soc.*, *Dalton Trans.*, 1994, 3211.